2024 IEEE 63rd Conference on Decision and Control (CDC)
December 16-19, 2024. MiCo, Milan, Italy

LPV Boost Pressure and EGR Rate Control of a Diesel Engine Air Charge System with eBoost Assistance

Corey Gamache[1], Guoming Zhu[1], and Tianyi He[2]

Abstract— **Turbocharged engines often suffer from significant intake manifold pressure response delay due to so-called turbo-lag. Many technologies have been investigated to combat this phenomenon, and combinations of them are often utilized together. The addition of these technologies to already complicated modern engines presents a significant control challenge due to significant system nonlinearity, especially when considering the large operating range of engine speeds and loads. In this paper, a model-based gain-scheduling control strategy is developed, utilizing a constrained $\mathcal{H}_2$ linear parameter-varying (LPV) control strategy, for the Ford 6.7L 8-cylinder diesel engine equipped with a variable geometry turbocharger (VGT), exhaust gas recirculation (EGR), and added eBoost along with a bypass valve. The nonlinear eBoost air charge system is modeled as a function of two scheduling parameters, engine load and bypass valve position, for this study and controllers are designed for the defined operating range of these parameters. The developed controller selection and interpolation scheme allows this strategy to be implemented onto computationally-limited hardware that cannot solve the controller, requiring matrix inverse calculation, online. The LPV control strategy is validated in both simulation and experimental studies, and the experimental results show a 66% reduction in engine response time in terms of reaching target intake manifold (boost) pressure following a load step-up, compared with the production configuration (without eBoost and bypass valve) with no significant impact on NOx emissions.**

I. Introduction

Today improving fuel efficiency and reducing greenhouse and pollutant emissions is a priority for vehicle manufacturers. Production diesel engines have adopted numerous technologies such as exhaust gas recirculation [1] and exhaust aftertreatment systems [2], [3] to realize these goals, and downsizing of engine displacement, adoption of forced induction, and electrification have brought additional improvements [4], [5]. Turbochargers, a form of forced induction, have been widely adopted but often introduce an intake manifold pressure, or boost, response delay that occurs between pressing the throttle and achieving the desired torque. This phenomenon is called “turbo-lag" [6], [7].

Numerous technologies have been investigated to reduce turbo-lag. Novel technologies such as VGTs can reduce turbo-lag but not eliminate it entirely [8]. Electrically-assisted turbochargers are another potential solution and come in several forms. In the case of the eTurbo, an electric motor is directly interfaced with the turbocharger’s turbine shaft, allowing it to augment the energy recaptured from the exhaust by the turbine with electrical energy [9], [10], or capture excess exhaust energy for regenerative braking [11]. Hydraulic turbo-assist works in the same manner, however additional energy is provided by high-pressure oil routed through a hydraulic drive system rather than an electric motor [12], [13]. Typically, these systems are not capable of recovering excess exhaust energy, however Tao, et al. [12], [13] have devised a system with such capability. External electrical compressor, or eBoost, systems [14] add a standalone compressor driven by an electric motor to the engine air charge plumbing. The eBoost may be placed either upstream or downstream of the turbocharger compressor depending on the desired performance benefits, where the upstream configuration is preferable for mid-speed and load operating conditions, and the downstream configuration is preferred elsewhere [14]. The comparatively fast dynamics of the eBoost compared to the turbocharger allows it to pressurize the intake air charge during the period in which the turbocharger alone cannot achieve the desired intake manifold pressure in transient operations. The eBoost is accompanied by a bypass valve that allows the intake air charge to be routed around the eBoost outside of transient operational conditions.

With the addition of these technologies, the air charge system control in modern engines has grown increasingly challenging, which has motivated research into model-based control strategies that may be better suited for complex MIMO systems than traditional single-input and single-output (SISO) strategies such as the widely used proportional-integral-derivative (PID) control. In reference [15], the PID control strategy was extended to control two actuators (VGT and waste-gate), called a dual PID controller, for boost pressure control, and in reference [16] the SISO dual PID controller (VGT and eBoost) was used for boost pressure regulation, while the EGR rate is controlled by another SISO PID controller for the diesel engine air charge system with eBoost. Modern model-based strategies such as $\mathcal{H}_\infty$, $\mathcal{H}_2$, LPV, and μ-synthesis-based control strategies have been developed for diesel engine air charge systems and have shown performance improvements as compared to traditional production strategies [17], [18], [19]. In reference [20] a switching linear quadratic tracking with integration (LQTI) control strategy is presented. Model predictive control (MPC) has also shown promise in improving performance over production calibrations [21].

In this paper, the challenge of air charge control with an eBoost upstream of the compressor and bypass valve is ad-

[1]C. Gamache and G. Zhu are with the Department of Mechanical Engineering, Michigan State University, East Lansing, MI 48824, USA (gamachec@msu.edu and zhug@msu.edu)

[2]Tianyi He is with the Department of Mechanical and Aerospace Engineering, Utah State University, Logan, UT 84322, USA (tianyi.he@usu.edu)

dressed through the development of an LPV control strategy with adjustable control gain for the VGT, EGR, and eBoost to handle system nonlinearity, especially the switching operation of the bypass valve. An operational mode transition logic is adopted for activating the eBoost and actuating the bypass valve; see reference [20] for details. For experimental validation, a controller selection and interpolation scheme for LPV control is additionally developed for implementing the LPV control strategy. The developed control strategy was validated in both simulation and experimental studies. The test results indicated a significant reduction of transient response time in terms of boost pressure with similar NOx emissions during step-up transitions and without increasing NOx emissions at steady-state operations, compared with those of the baseline production control scheme, which utilizes two SISO PID controllers for the VGT and EGR valves to control boost pressure and EGR rate, respectively.

The main contributions of this paper are three-fold: a) developing an eBoost LPV strategy and controller selection and interpolation scheme for coordinated control of boost pressure and EGR rate for an engine air charge system equipped with an eBoost and its bypass valve, b) modifying the existing $\mathcal{H}_2$ LPV control conditions for output covariance constraint (OCC) [22] LPV control to make possible LPV control gain tuning, and c) validating the proposed strategy experimentally to demonstrate the performance improvement of using the OCC LPV control of the eBoost system with discrete bypass valve for a diesel engine air charge system over the existing production engine control strategy without eBoost.

This paper is organized as follows. The next section describes a nonlinear model for the diesel engine air charge system with eBoost and development of the LPV model, followed by a section detailing the LPV control design process, then a section describing the simulation and experimental setup and results. Finally, concluding remarks are given in the last section.

II. Air flow system model with a discrete valve

The nonlinear diesel engine air charge model with eBoost and bypass valve was originally developed by Yifan Men in [14], and was further modified in [20]. The nonlinear state equations for pre-compressor pressure, intake manifold pressure, exhaust manifold pressure, and turbocharger shaft speed are shown below by (1) to (4), respectively.

$$\dot{p}_1 = \frac{RT_1}{V_1}\left(\dot{m}_e + \dot{m}_{bp} - \dot{m}_c\right) \tag{1}$$

$$\dot{p}_2 = \gamma\frac{R}{V_2}\left(\dot{m}_c T_{cac} + \dot{m}_{egr} T_{egr} - \dot{m}_{in} T_2\right) \tag{2}$$

$$\dot{p}_3 = \gamma\frac{R}{V_3}\left(\dot{m}_{out} T_{out} - \dot{m}_{egr} T_3 - \dot{m}_t T_3\right) \tag{3}$$

$$\dot{\omega}_{tc} = \frac{1}{J_c \omega_{tc}}\left(\dot{W}_t - \dot{W}_c - \dot{W}_l\right) \tag{4}$$

where γ is the heat capacity ratio, R is the ideal gas constant, J_c is the turbocharger compressor moment of inertia, T_{cac} is the intake charge air cooler outlet temperature, T_{egr} is the EGR cooler outlet temperature, T_{out} is the engine exhaust temperature, $\dot{W}_t$ is the turbocharger turbine power, $\dot{W}_c$ is the turbocharger compressor power, and $\dot{W}_l$ is the mechanical power loss of the turbocharger shaft. The air charge system diagram with definition of all variables can be found in Fig. 1. Note that EGR rate is defined by (5).

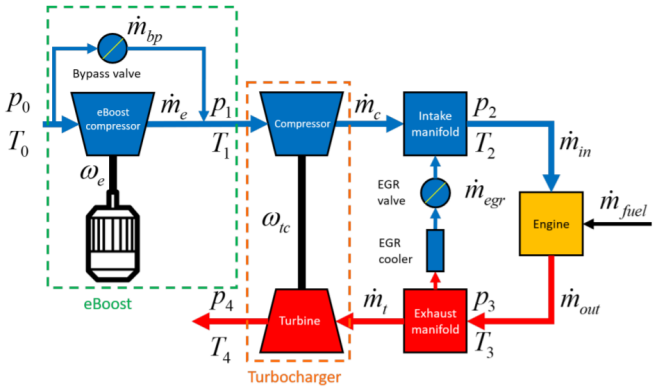

Fig. 1: Air charge system with an eBoostand bypass valve

$$EGR\ rate = \frac{\dot{m}_{egr}}{\dot{m}_{egr} + \dot{m}_c} \tag{5}$$

Additionally, actuator dynamics for the VGT and EGR valve were approximated with first-order transfer functions using experimental data. The VGT and EGR valve position states (pos_{VGT}, pos_{EGR}) were augmented with the original four-state nonlinear model ((1) to (4)), resulting in a six-order nonlinear model of the following form.

$$\dot{x}_n = f(x_n, u, w_2) \tag{6}$$

$$z = g_z(x_n) \tag{7}$$

where $z = [p_2, EGR\ rate]^T$ is the system performance output vector, and w_2 is the system input noise. Both nonlinear state (x_n) and control input (u) vectors are defined below.

$$x_n = [\ pos_{VGT},\ pos_{EGR},\ p_1,\ p_2,\ p_3,\ w_{tc}\ ]^T \tag{8}$$

$$u = [VGT_{cont}, EGR_{cont}, eBoost_{speed}, pos_{bypass}]^T \tag{9}$$

Note that VGT_{cont}, EGR_{cont}, $eBoost_{speed}$, and pos_{bypass} are control inputs to the nonlinear system for VGT, EGR valve, eBoost reference speed, and bypass valve position, respectively. The bypass valve is a treated as a discrete valve, thus aside from brief moments of transient movement between the two positions, it is operated as a discrete valve (open or closed). The open-closed operation introduces significant challenge for the control strategy due to changing dynamics and nonlinearity during the transition. Note that the bypass valve on-off operation is determined by the engine throttle input as described in [16].

Two scheduling parameters are used: α and β, for the engine load and bypass valve position, respectively. Engine load is chosen as the first scheduling parameter because the air charge system dynamics change significantly with load for a given engine speed. In [20], the authors concluded a

single controller designed at a median load condition for a given engine speed could not provide adequate performance across the entire range of typical engine loads. The engine driving cycle of interest features load ranging from 2 to 5 BMEP. For this study, the engine load scheduling parameter is α, where $\alpha = 0$ is associated with 3 BMEP and $\alpha = 1$ is with 4 BMEP. It is assumed that the controllers for $\alpha = 0$ are valid for load values as low as 2 BMEP and the $\alpha = 1$ controllers for up to 5 BMEP. For future work, the full range of engine loads will be considered.

Bypass valve position is chosen as the second scheduling parameter because the air charge system with the bypass valve open mimics the existing production setup and only uses two control actuators (VGT and EGR), whereas with the bypass valve closed the system uses three actuators (eBoost, VGT, and EGR). Note that the eBoost is only enabled when the bypass valve is closed. The system dynamics are thus quite different when the valve is open versus closed since use of the eBoost allows for quicker intake manifold pressure response than the VGT alone [16], [20]. For the bypass valve position scheduling parameter, β, $\beta = 0$ is associated with the bypass valve open, and $\beta = 1$ with the bypass valve closed.

The scheduling parameters are thus unit simplex variables,

$$\Lambda : \ 0 \leq \theta_i(t) \leq 1, \ i = 1, 2, \tag{10}$$

where θ is the vector of scheduling parameters, $\theta = [\alpha, \beta]^T$. The scheduling parameter rates of changes are also assumed to be uniformly bounded in the positive and negative directions,

$$\Omega : \ -\nu_{\theta_i} \leq \dot{\theta}_i(t) \leq \nu_{\theta_i}, \ i = 1, 2. \tag{11}$$

Note that we are going to denote the set described by (10) and (11) by $(\theta, \dot{\theta}) \in \Lambda \times \Omega$. The open-loop affine LPV system is then defined as

$$\Sigma(\theta) \ : \ \begin{cases} \dot{x}(t) = A(\theta(t))x(t) + B_2(\theta(t))w_2(t) \\ \qquad\qquad + B_u(\theta(t))u(t) \\ z_2(t) = C_2(\theta(t))x(t) \end{cases} \tag{12}$$

where $\theta = [\theta_1, \theta_2]^T = [\alpha, \beta]^T$, $x(t) \in \mathbf{R}^6$ is the state vector, $w_2(t) \in \mathbf{R}^3$ the $\mathcal{L}_2$ disturbance input, $u(t) = [VGT, EGR, eBoost]^T \in \mathbf{R}^3$ the control input, and $z_2(t) = [p_2, EGRrate]^T \in \mathbf{R}^2$ the $\mathcal{H}_2$ performance output. Again, note that the bypass valve is controlled by the transition logic described in [16].

For LPV controller generation as discussed in the following section, four corner-point linearized models were found corresponding with α and β values of $[0, 0]$, $[0, 1]$, $[1, 0]$, and $[1, 1]$, respectively. A balanced realization for the $\alpha = 0, \beta = 0$ model was found with balanced transformation matrices T_L and T_R such that

$$A_b(\theta(t)) = T_L A(\theta(t)) T_R \tag{13}$$

$$B_b(\theta(t)) = T_L B_2(\theta(t)) \tag{14}$$

$$C_b(\theta(t)) = C_2(\theta(t)) T_R \,, \tag{15}$$

where A_b, B_b, and C_b are system matrices in the balanced coordinates. The same T_L and T_R matrices were then used to balance the three remaining corner-point models.

Finally, the parameter vector, θ, must be mapped into a multi-simplex domain to perform convex analysis. The multi-simplex domain is defined as the Cartesian product of multiple unit-simplex variables, and the remapping of each parameter to a unit simplex follows the process in [23], which is simplified for the case where $\theta_i \in [0, 1]$,

$$\lambda_{i,1} = \theta_i(t) \,, \quad \lambda_{i,2} = 1 - \lambda_{i,1} \tag{16}$$

resulting in $\lambda_i = (\lambda_{i,1}, \lambda_{i,2}) \in \Lambda_{i,2}$, where $\Lambda_{i,2}$ is the two-dimensional unit simplex. The system $\Sigma(\lambda)$ is assumed to be of the same form as $\Sigma(\theta)$ with system matrices that are functions of λ. Note that the scheduling parameters are remapped back to the affine domain of θ for controller implementation.

III. LPV CONTROL AND DESIGN

Using the methods described in [23], a gain-scheduling state-feedback controller of the form

$$u(t) = [u_1(t), u_2(t), u_3(t)]^T = K(\lambda(t))x(t), \tag{17}$$

can be designed, then substituting (17)) into (12) yields the closed-loop LPV system

$$\Sigma_{cl}(\lambda) : \begin{cases} \dot{x}(t) = A_{cl}(\lambda)x(t) + B_2(\lambda)w_2(t); \\ z_2(t) = C_2(\lambda)x(t) \end{cases} \tag{18}$$

The objective of the OCC control design (see [22] for details), resulting in an $\mathcal{H}_2$ controller, is to find a state-feedback gain-scheduling controller ((17)) for the LPV system ((12)) that minimizes the following $\mathcal{H}_2$ performance cost

$$\min_{K(\lambda)} trace(Q\bar{U}) \,, \tag{19}$$

such that the closed-loop system ((18)) is exponentially stable and the following constraints are satisfied,

$$C_2(1,:)WC_2^T(1,:) \leq \sigma_1 \tag{20}$$

$$C_2(2,:)WC_2^T(2,:) \leq \sigma_2 \,, \tag{21}$$

where σ_k $(k = 1, 2)$ are the given constraints on the upper bound of output covariance W, where $W \geq Cov(C_2x(t))$. By varying parameters σ_1 and σ_2, e.g. gradually relaxing the output covariance constraints, a family of controllers can be generated with control gains from low to high, which can be used for control gain tuning. For each pair of covariance constraints, the controller

$$K(\lambda) = Z(\lambda)G^{-1}(\lambda) \tag{22}$$

is found using the theorem detailed in [23] and modified for the OCC problem as below, where the cost function is modified for the OCC problem to be the weighted control energy

$$\min trace(Q\bar{U}) \,, \tag{23}$$

so that given the output covariance constraints σ_k, $(k = 1, 2)$ is satisfied if there exists a continuously differentiable

parameter-dependent matrix $0 < P_2(\lambda) = P_2^T(\lambda) \in \mathbf{R}^{6\times 6}$, $G(\lambda) \in \mathbf{R}^{6\times 6}$, $Z(\lambda) \in \mathbf{R}^{3\times 6}$, small scalars $\epsilon_2 > 0$, and matrix $W = W^T \in \mathbf{R}^{2\times 2}$ that minimizes the cost function with a given scaling matrix $Q > 0$ subject to the following parameterized linear matrix inequalities (LMIs) ($*$ denotes symmetric terms),

$$\begin{bmatrix} \Phi_{11} & * & * \\ \Phi_{12} & -\epsilon_2(G(\lambda)+G(\lambda)^T) & * \\ B_2(\lambda)^T & \mathbf{0}_{3\times 3} & -\mathbf{I}_3 \end{bmatrix} < 0\,, \quad (24)$$

$$\begin{bmatrix} W & C_2(\lambda)G(\lambda) \\ * & G(\lambda)+G(\lambda)^T - P_2(\lambda) \end{bmatrix} > 0\,, \quad (25)$$

$$\begin{bmatrix} \bar{U} & Z(\lambda) \\ * & G(\lambda)+G(\lambda)^T - P_2(\lambda) \end{bmatrix} > 0, \quad (26)$$

where $\Phi_{11} = A(\lambda)G(\lambda) + B_u(\lambda)Z(\lambda) + (A(\lambda)G(\lambda) + B_u(\lambda)Z(\lambda))^T - \frac{\partial P_2(\lambda)}{\partial \lambda}\dot{\lambda}$, and $\Phi_{12} = P_2(\lambda) - G(\lambda) + \epsilon_2(A(\lambda)G(\lambda)+B_u(\lambda)Z(\lambda))^T$, then the gain-scheduling controller

$$u(t) = K(\lambda)x(t)\,,\ K(\lambda) = Z(\lambda)G^{-1}(\lambda) \quad (27)$$

exponentially stabilizes the LPV system $\Sigma(\lambda)$ in (12) for any $(\lambda, \dot{\lambda}) \in \Lambda \times \Omega$; see [23] for further detail. In addition, the OCC cost (23) is minimized and output covariance constraints (20) are satisfied such that

$$\sigma_1 - C_{2,1}WC_{2,1}^T \geq 0 \quad (28)$$

$$\sigma_2 - C_{2,2}WC_{2,2}^T \geq 0\,. \quad (29)$$

Initial values for σ_1 and σ_2 were found as described in reference [20], and $Z(\lambda)$ and $G(\lambda)$ are selected to be of affine structure. By iteratively generating controllers for increasingly relaxed values of σ_1 and σ_2 a family of controllers with gains from high to low were generated. For this investigation, the matrix coefficient check relaxation approach [24] was used to solve the developed PLMIs in (24) through (28) in the multi-simplex domain, and the optimization problem was solved using the ROLMIP [25] and YALMIP [26] packages for Matlab and solver SeDuMi [27].

IV. Simulation and Experimental Results

The experimental setup used is as described in [20], with the additional software modification to allow for use of the same EGR rate reference and feedback signals from the OEM PCM (powertrain control module) with the EGR valve connected or disconnected from the production wiring harness. This was required to equivalently compare the air charge system responses of the LPV control strategy with the production control scheme because the EGR valve is disconnected from the production wiring harness when the LPV strategy is being used; see [16] for details of the experimental setup. The recorded control response data was advanced by one sample (100 ms) in the plots to account for the averaged control area network (CAN) communication delay and data recording frequency of 10 Hz for all signals dependent on communication among the production PCM, MotoTron (where the LPV controller is implemented), and NI data recording system. The eBoost was run at a minimum speed of 10,000 RPM at all times when the LPV strategy was used to avoid a response delay in the prototype eBoost system due to an issue with the prototype control unit that caused up to a 200 ms delay when initially accelerating the eBoost from below 10,000 RPM. This workaround was required to achieve fast eBoost response during transient events. This issue could be fixed by the eBoost supplier by reprogramming the eBoost controller. The experimental results are discussed below, where the response time given is calculated starting from the time of load step to when the actual value reaches a $\pm 10\%$ error band and stays within this error band (i.e., 10% settling time) as shown in (30) below.

$$p_{2,actual} \in [0.9\Delta p_{2,target}, 1.1\Delta p_{2,target}] \quad (30)$$

where $\Delta p_{2,target}$ is the incremental target change of p_2.

Due to the processing constraints of the MotoTron control module used, the controller $K(\theta)$ could not be calculated online as a function of the scheduling parameters α and β. The MotoTron has similar processing capability and memory capacity as many common production PCMs, thus the control strategy must be able to run on the MotoTron to be considered viable for production. To accomplish this, a controller selection logic was developed to choose one or a combination of 16 controllers that were calculated offline using combinations of $\alpha = 0, 0.5, 0.75, 1$ and $\beta = 0, 0.5, 0.75, 1$. These values were chosen because the system dynamics are close to linear for values of α or β between 0 and 0.5, and become more nonlinear from 0.5 to 1. This 16 controller interpolation strategy provides close performance to that of calculating $K(\theta)$ with much less computational complexity and acceptable memory requirements. These controllers form a two-dimensional grid associated with values of α and β from 0 to 1. The scheduling parameters are then calculated online, and used to determine which controller or interpolated combination of controllers from the 4x4 grid to use. Fig. 2 illustrates the four controllers, marked in red, of the 16 total controllers, marked with black circles, to be interpolated for an example (α, β) operating condition marked in blue.

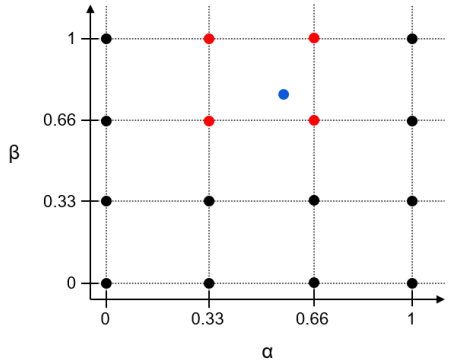

Fig. 2: 4x4 grid of LPV controllers for α and $\beta \in [0, 1]$

The LPV control strategy was first validated in simulations using the linearized model, then on the six-state nonlinear

model in (6). Fig. 3 shows the simulated response for a 3 to 4 BMEP ($\alpha = 0$ to 1) using the nonlinear air charge model. It was then programmed onto the experimental setup and experimentally validated.

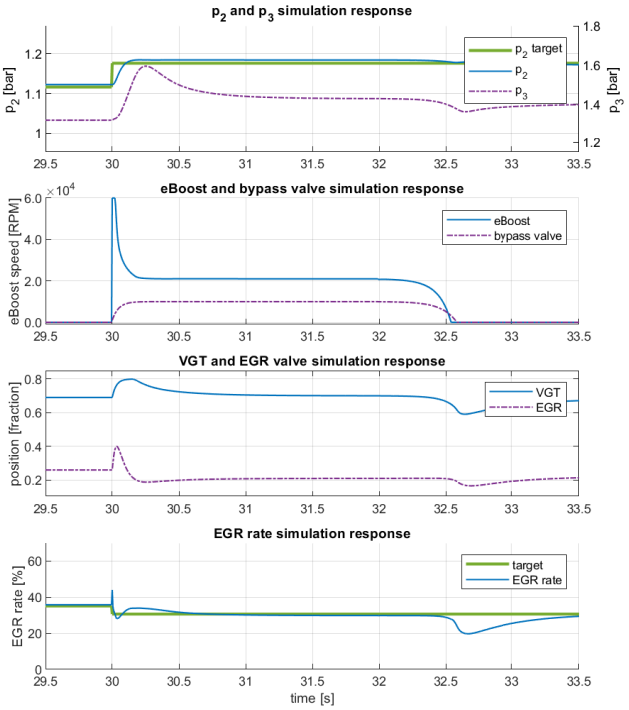

Fig. 3: Simulated LPV responses for 3 to 4 BMEP step

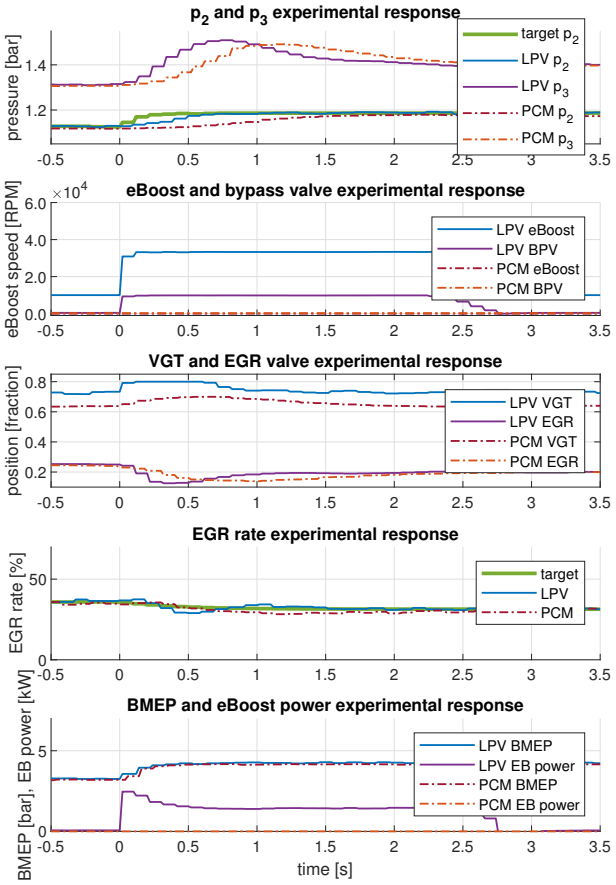

Fig. 4: Experimental LPV responses for 3 to 4 BMEP step

Fig. 4 shows a comparison of a typical experimental step-up response from 3 to 4 BMEP, corresponding to $\alpha = 0$ to 1, step-up using the proposed LPV control strategy with that of the production control strategy without eBoost. Note that β varies from 0 to 1 to 0 as the bypass valve briefly closes then opens during the transient event. For this step-up the LPV strategy improves response time in terms of intake manifold pressure by 66% with an additional dip of EGR rate response, comparing with the production response, but recovered quickly, which leads to similar NOx emissions during transient operation. Integrated p_2 error is reduced from 0.072 bar·s to 0.027 bar·s during the load step up using the LPV control strategy. Note some steady-state error exists due to the lack of integration terms in the controller. Fig. 5 shows the response for a step down from 4 to 3 BMEP ($\alpha = 1$ to 0). Response in this case is similar to the production strategy since the eBoost only aids with load increments, not during load decrements.

V. Conclusion

An eBoost and bypass valve were added to a production Ford 6.7L diesel engine to improve its transient intake manifold pressure response. An OCC LPV control strategy was proposed, developed, and validated in simulations and experimentally to reduce engine turbo-lag without increasing NOx emissions. Due to the limited computational capability of the MotoTron control module used, a controller selection and scheduling scheme was developed to allow implementation of the LPV control strategy for the MIMO nonlinear air charge system onto the experimental test stand. The experimental results showed a 66% improvement in intake manifold pressure response speed compared to the production control strategy without eBoost. This paper illustrates the potential of the proposed LPV control strategy to improve transient performance in terms of intake manifold pressure response across a range of operating conditions, without negatively effecting NOx emissions. The next steps for this work are first, to gradually increase the gain of the controllers to better leverage the eBoost and further improve performance, and second, to increase the range of operating conditions. Future work may include adding engine speed as an additional scheduling parameter, alongside α and β, to increase the operating range of the strategy across both engine load and speed. Finally, the future addition of integration terms for intake manifold pressure and EGR rate to eliminate steady-state errors is recommended.

References

[1] M. J. van Nieuwstadt, I. V. Kolmanovsky, and P. E. Moraal, "Coordinated egr-vgt control for diesel engines: an experimental comparison," *SAE Transactions*, vol. 109, pp. 238–249, 2000. [Online]. Available: http://www.jstor.org/stable/44634217

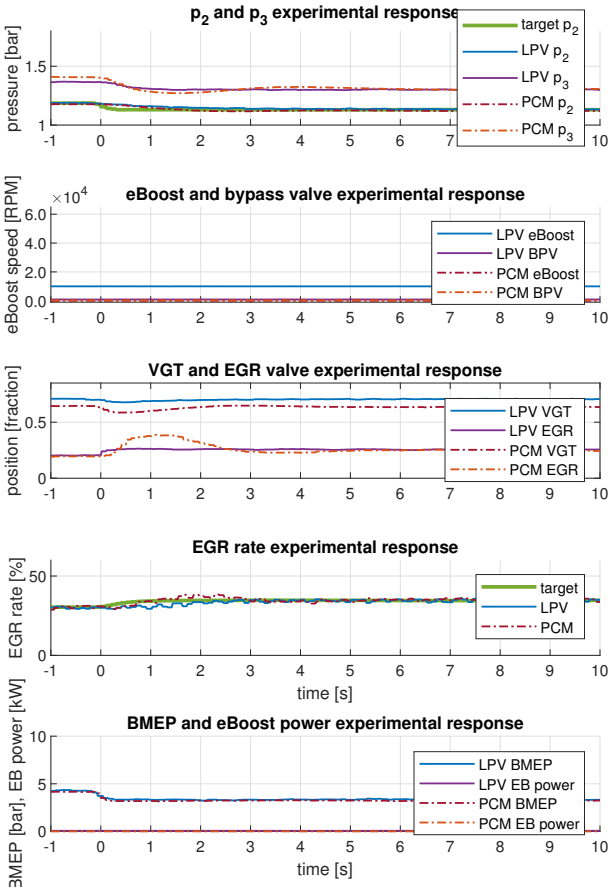

Fig. 5: Experimental LPV responses for 4 to 3 BMEP step

[2] B. Apicella, E. Mancaruso, C. Russo, A. Tregrossi, M. M. Oliano, C. Anna, and B. M. Vaglieco, "Effect of after-treatment systems on particulate matter emissions in diesel engine exhaust," *Experimental Thermal and Fluid Science*, vol. 116, no. 08, p. 110107, 2020.

[3] J. Chi, "Control challenges for optimal nox conversion efficiency from scr aftertreatment systems," *SAE Technical Papers 2009-01-0905,*, 2009.

[4] J. M. Mazanec, N. S. Vang, and S. L. Kokjohn, "Enabling off-highway diesel engine downsizing and performance improvement using electrically assisted turbocharging," *International Journal of Engine Research*, vol. 24, no. 9, pp. 4104–4126, 2023. [Online]. Available: https://doi.org/10.1177/14680874231181002

[5] J. Yi, S. Wooldridge, G. Coulson, J. Hilditch, C. O. Iyer, P. Moilanen, G. Papaioannou, D. Reiche, M. Shelby, B. VanDerWege, C. Weaver, Z. Xu, G. Davis, B. Hinds, and A. Schamel, "Development and optimization of the ford 3.5l v6 ecoboost combustion system," *SAE International Journal of Engines*, vol. 2, no. 1, pp. 1388–1407, 2009.

[6] H. Stoffels, S. Quiring, and B. Pingen, "Analysis of transient operation of turbo charged engines," *SAE International Journal of Engines*, vol. 3, no. 2, pp. 438–447, 2010.

[7] I. V. Kolmanovsky, M. J. V. Nieuwstadt, and P. E. Moraal, "Method of reducing turbo lag in diesel engines having exhaust gas recirculation," *US Patent, US6178749B1*, 2001.

[8] A. J. Feneley, A. Pesiridis, and A. M. Andwari, "Variable geometry turbocharger technologies for exhaust energy recovery and boosting-a review," *Renewable and Sustainable Energy Reviews*, vol. 71, pp. 959–975, 2017. [Online]. Available: https://www.sciencedirect.com/science/article/pii/S1364032116311807

[9] T. Katrašnik, S. Rodman Opresnik, F. Trenc, A. Hribernik, and V. Medica, "Improvement of the dynamic characteristic of an automotive engine by a turbocharger assisted by an electric motor," *Journal of Engineering for Gas Turbines and Power-transactions of The Asme - J ENG GAS TURB POWER-T ASME*, vol. 125, 04 2003.

[10] E. Winward, J. Rutledge, J. Carter, A. Costall, R. Stobart, D. Zhao, and Z. Yang, "Performance testing of an electrically assisted turbocharger on a heavy duty diesel engine," 05 2016.

[11] P. Dimitriou, R. Burke, Q. Zhang, C. Copeland, and H. Stoffels, "Electric turbocharging for energy regeneration and increased efficiency at real driving conditions," *Applied Science*, vol. 7, no. 350, 2017.

[12] T. Zeng, D. Upadhyay, H. Sun, E. Curtis, and G. G. Zhu, "Regenerative hydraulic assisted turbocharger," in *Proceedings of ASME Turbo Expo 2017: Turbomachinery Technical Conference and Exposition*, vol. GT2017. ASME, 2017.

[13] T. Zeng, D. Upadhyay, and G. Zhu, "Modeling and control of a diesel engine with regenerative hydraulic assisted turbocharger," *ASME Journal of Dynamic Systems, Measurement, and Control*, vol. 144, no. 5, pp. 051 004–1, 2019.

[14] Y. Men, "Reaction-based modeling and control of an electrically boosted diesel engine," Ph.D. dissertation, Michigan State University, 2019.

[15] G. G. Zhu, M. W. Pyclik, E. K. Bradley, and L. J. Brackney, "Closed-loop actuator control system having bumpless gain and anti-windup logic," U.S. Patent 6 424 906, 2002.

[16] C. Gamache, M. V. Nieuwstadt, J. Martz, and G. Zhu, "Dual-output pid transient control of an electric-assisted air charge system," *International Journal of Engine Research*, vol. 24, no. 8, pp. 3519–3531, 2023. [Online]. Available: https://doi.org/10.1177/14680874231154964

[17] M. Lee and M. Sunwoo, "Model-based control of a diesel engine variable geometry turbine and exhaust gas recirculation system using a linear parameter varying methodology," *Proceedings of the Institution of Mechanical Engineers, Part D: Journal of Automobile Engineering*, vol. 228, no. 14, pp. 1633–1643, 2014. [Online]. Available: https://doi.org/10.1177/0954407012465069

[18] W. Qiu, S. H. Rayasam, G. M. Shaver, T. G. Rimstidt, and D. G. V. Alstine, "Control design-oriented modeling and μ-synthesis-based robust multivariate control of a turbocharged natural gas genset engine," *International Journal of Engine Research*, vol. 24, no. 9, pp. 3905–3921, 2023. [Online]. Available: https://doi.org/10.1177/14680874231177748

[19] S. H. Rayasam, W. Qiu, T. Rimstidt, G. M. Shaver, and D. G. V. Alstine, "Robust model-based switching mimo air handling control of turbocharged lean-burn si natural gas variable speed engines," *International Journal of Engine Research*, vol. 24, no. 6, pp. 2783–2804, 2023. [Online]. Available: https://doi.org/10.1177/14680874221134318

[20] C. Gamache, M. V. Nieuwstadt, J. Martz, and G. Zhu, "Lqti boost pressure and egr rate control of a diesel air charge system with eboost assistance," *International Journal of Engine Research*, vol. 0, no. 0, p. 14680874231154964, 0.

[21] M. Huang, D. Liao-McPherson, S. Kim, K. Butts, and I. Kolmanovsky, "Toward real-time automotive model predictive control: A perspective from a diesel air path control development," in *2018 Annual American Control Conference (ACC)*, 2018, pp. 2425–2430.

[22] G. Zhu, M. Rotea, and R. E. Skelton, "A convergent algorithm for the output covariance constraint control problem," *SIAM Journal on Control and Optimization*, vol. 35, no. 1, pp. 341–361, Jan 1997.

[23] T. He, A. K. Al-Jiboory, G. G. Zhu, S. S.-M. Swei, and W. Su, "Application of icc lpv control to a blended-wing-body airplane with guaranteed h-infinity performance," *Aerospace Science and Technology*, vol. 81, pp. 88–98, 2018. [Online]. Available: https://www.sciencedirect.com/science/article/pii/S1270963817318710

[24] R. C. L. F. Oliveira, P. Bliman, and P. L. D. Peres, "Robust LMIs with parameters in multi-simplex: existence of solutions and applications," in *47th IEEE Conference on Decision and Control*, Dec 2008, pp. 2226–2231.

[25] C. M. Agulhari, R. C. L. F. Oliveira, and P. L. D. Peres, "Robust LMI parser: a computational package to construct LMI conditions for uncertain systems," in *XIX Brazilian Conference on Automation (CBA 2012)*, Campina Grande, PB, Brazil, 2012, pp. 2298–2305.

[26] J. Löfberg, " YALMIP : A toolbox for modeling and optimization in MATLAB," in *Proceedings of the CACSD Conference*, Taipei, Taiwan, Sep 2004, pp. 284–289.

[27] J. Sturm, "Using SeDuMi 1.02, a MATLAB toolbox for optimization over symmetric cones," *Optimization Methods and Software*, vol. 11, no. 1, pp. 625–653, 1999.